Journal of Advanced Manufacturing Science and Technology 5(3) (2025) 2025016

Journal of
Advanced Manufacturing Science and Technology
jamst@jamstjournal.com;jamst2020@126.com
www.jamstjournal.com

Experimental study on robot laser and side-milling compound technology for drilling of CFRP/TC4 laminated stacks

Wenjie LV[a], Song DONG[a], Mingzhu YUAN[b], Zhenwen SUN[a], Xin WANG[a], Kan ZHENG[a,*]

[a]*School of Mechanical Engineering, Nanjing University of Science and technology, Nanjing 210094, China*
[b]*Shanghai Institute of Space craft Equipment, Shanghai 200240, China*

Received 10 September 2024; revised 6 October 2024; accepted 8 November 2024; Available online 28 November 2024

Abstract: Aiming at the problems of low efficiency and serious tool wear in the drilling large hole for aviation large and complex carbon fiber reinforced polymer (CFRP)/titanium alloy (TC4) laminated stacks, a new process of robot laser and side-milling compound drilling is proposed, which has the advantages of high surface quality, high precision of geometry and high efficiency. laser and side-milling compound drilling experiment of CFRP/TC4 laminated stacks was carried out, and the effect of process parameters on the processing quality was explored. A ∅15 mm high precision hole was drilled on an 8mm CFRP/TC4 laminated stacks. Experimental results show that laser-induced heat affected zone (HAZ) can greatly reduce the cutting force during the milling process, the average cutting force of CFRP is reduced by 60.8%, and the average cutting force of TC4 is reduced by 66.2%. The introduction of minimal quantity lubrication (MQL) can greatly improve the surface quality. The surface roughness (Sa) of CFRP and TC4 decreasing by 36.1% and 36.8%, respectively, compared with dry cutting, and both remaining below 3.2 μm. The minimum interlayer burrs of CFRP and TC4 are 26.734 μm and 60.802 μm respectively.

Keywords: CFRP/TC4 laminated stacks; robotic compound technology for drilling; heat affected zone; surface roughness; tool wear

1. Introduction

CFRP/TC4 laminated stacks are widely used in the aviation structures due to their excellent specific strength and stiffness. [1-6] A large number of rivet and threaded holes need to be made on large components before the assembly process of laminated stacks, particularly for large civil aircraft like C919, C929 and Airbus A380, which need various types of holes. Among these, tens of thousands of holes have diameters greater than 10 mm. Currently, robotic drilling technology is widely used in the aircraft assembly process by aviation manufacturing enterprises. However, when robots are used to drill large holes, flutter is prone to occur due to excessive axial force, which severely affects the hole quality and accuracy. [7-11] Additionally, the cutting temperature is becomes extremely high during the dry cutting of TC4 in an open environment, causing the CFRP matrix to soften and increasing the risk of delamination damage. [12-17] As a result, it is difficult to meet the high precision and high quality requirements of connecting holes in the field of aviation manufacturing.

To address the challenge of achieving high precision and quality in drilling CFRP/TC4 laminated stacks, some scholars have proposed using helical milling to drill. Helical milling creates circular holes by eccentric milling. At the same time, high precision and high quality large holes can be achieved at one time by adjusting the eccentricity. Compared with the traditional drilling process, it offers advantages such as better processing quality, high efficiency and low tool wear. [18-20] However, the cutting width in helical milling is typically equal to the tool diameter, resulting in full cutting width. This can generate excessive cutting forces, leading to flutter in the workpiece and the robot. [21-22] Therefore, the helical milling process is typically performed in high-speed machining center or three-axis linkage milling machine, which cannot be directly applied to industrial robots. At the same time, some scholars have presented to use the advantages of laser processing in tool wear, cutting force and processing efficiency to drill. [23-25] But the defects in the HAZ caused by laser processing will reduce the mechanical properties of the material and significantly impact its service life. [26-29] Consequently, the formation of the HAZ in laser drilling significantly hinders its broader application. However, as of today, these challenges remain unresolved.

Therefore, based on the advantages of high efficiency of laser processing and high precision of milling, aiming at the problem of drilling large holes in large and complex laminated stacks, this pa-

* Corresponding author. *E-mail address:* zhengkan@njust.edu.cn(Kan ZHENG)
Peer review under responsibility of Editorial Committee of JAMST
DOI: 10.51393/j.jamst.2025016

per proposes a new process of robot laser and side-milling compound technology for drilling. CFRP/TC4 laminated stacks are selected for laser drilling and side-milling reaming experiments. The relationship between laser parameters, HAZ and milling force is analyzed. Additionally, the hole processing quality under dry cutting and minimum quantity lubrication (MQL) conditions is compared. These findings offer valuable insights for drilling large holes in aviation laminated components.

2. Experimental design

2.1. Experiments platform setup

The KUKA robot processing system is selected as the experimental platform. The laser equipment is a high power fiber continuous laser YDFL-15000-CW-MM, which be installed on the end of KUKA-KR16 robot through flange during the experiment of laser. The specific parameters of the laser processing system are shown in Table 1. During the experiment, air was used as an auxiliary gas and was applied to the surface of the workpiece through a nozzle coaxial with the laser beam. The side-milling reaming experiment was conducted using the KUKA KR500 robot equipped with an end effector. The end effector is equipped with a 9105-NET-Omega160 six-axis force / torque sensor, which can collect the cutting force during the milling process. The milling tool is a ∅8 mm diamond end milling cutter, and MQL is used for cooling and lubrication during the milling process. The experiments platform of side-milling reaming experiment is shown in Fig. 1. During the experiment, the workpiece remained stationary. The relative positions of the two robots used in the laser and milling experiments, along with the workpiece, were recreated in DELMIA software. The robots were programmed offline in the software to achieve precise hole positioning.

Table 1 Parameters of YDFL-15000-CW-MM fiber laser.

Parameter	Unit	Value
Center wavelength	nm	1070-1090
Output power	W	0-15000
Core diameter	μm	100
Maximum modulation frequency	kHz	100
Nozzle diameters	mm	5
Gas pressure	bar	0-20

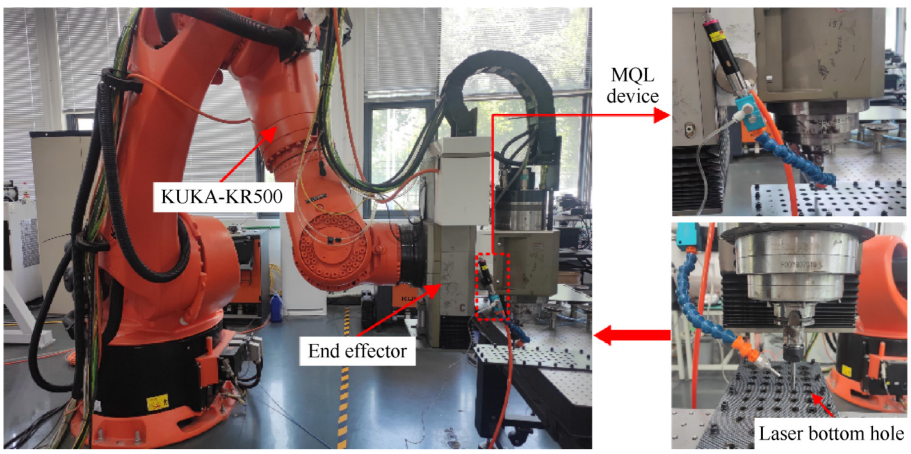

Fig. 1. Experimental platform of side-milling experiment with MQL.

The CFRP used in the test has an orthogonal structure of 0° and 90°, with T300 epoxy resin as the matrix material. The material properties of CFRP and TC4 alloy are shown in Table 2 and Table 3. Both the CFRP and TC4 have a thickness of 4 mm. During the experiment, the CFRP and TC4 were fixed together using bolts.

Table 2 Mechanical-physical properties of CFRP.

Parameter	Unit	Carbon fiber	Resin matrix
Density	kg/m^3	1850	1250
Thermal conductivity	W/(m·K)	Axial 5,Radial 50	0.2
Specific heat capacity	J/(kg·K)	710	1200
Steaming temperature	K	3500	425
Young's modulus	GPa	230	8.4

Table 3 Mechanical-physical properties of TC4.

Parameter	Unit	Value
Density	g/cm^3	4.43
Yield strength	MPa	935
Tensile strength	MPa	1014
Elastic modulus	GPa	110
Poisson ratio		0.34

2.2. Experiments scheme

Considering the high reflectivity of TC4, if processed in the order from TC4 to CFRP, part of the laser energy will be reflected and cannot be effectively transmitted into the material, reducing the processing efficiency and quality. At the same time, based on the structural characteristics of the metal skeleton and CFRP skin of the aviation device, as well as the actual processing methods used in engineering. In this paper, the processing sequence from CFRP to TC4 is used to carry out experimental research. The entire drill is divided into two stages. The first stage (laser rough machining), a ∅ 9 mm base hole was created through one-pass ring cutting using a high-power continuous laser. The second stage (side-milling reaming), multiple milling operations were performed on the base hole, and only a certain thickness of the material is milled each time to expand the hole layer by layer until a complete through hole is made.

A large number of preliminary experiments show that the test pieces are difficult to cut through with the laser at low power and high cutting speeds. Therefore, appropriate laser processing parameters were selected, as shown in Table 4. In addition, in the side-milling stage, significant damage of CFRP such as burr and delamination is observed at low speed, and the rapid accumulation of cutting heat in TC4 at high speed resulted in poor processing quality.

Consequently, the spindle speed range for the side-milling stage was set to 4000-7000 r/min. In view of the difficult processing characteristics of TC4, the cutting depth range was chosen to be 0.1-0.4 mm. The single factor experiment scheme is shown in Table 5.

Table 4 Experimental parameters of laser drilling.

Laser power(W)	Cutting speed ($m \cdot min^{-1}$)	Gas pressure (bar)	Nozzle height (mm)
9000			
10000			
11000			
12000	0.4/0.6/0.8/1.0	20	0.5
13000			
14000			
15000			

Table 5 Experimental parameters of side-milling reaming

Spindle speed($r \cdot min^{-1}$)	Feed rate ($mm \cdot min^{-1}$)	Axial cutting Depth(mm)	Cutting width (mm)
4000			
5000	120	0.1/0.2/0.3/0.4	1
6000			
7000			

In order to compare the influence of processing parameters on the surface quality of hole, three regions on the surface of the hole wall of the specimen were observed using a laser microscope (KEYENCE, VK-100 series). Five areas of 100 μm×100 μm were selected in each regions to measure the roughness of the hole wall. In order to ensure the reliability of the experiment, each set of parameters were repeated five times, and the experimental results were averaged.

3. Experimental results

3.1. Analysis of laser thermal damage change

After laser cutting, the morphology of the material changes due to the influence of laser. Therefore, the area where the surface morphology of the workpiece changes significantly is considered the HAZ, as shown in Fig. 2(a) and (b). The size of the HAZ is measured by magnifying the surface of the workpiece through laser microscope, and observing the width from the boundary where the surface morphology remains unchanged to the edge of the kerf. To analyze the size of HAZ after laser drilling, the defect factor method is used to characterize the size of HAZ with the damage factor F_d, which is defined as

$$F_d = \frac{D_{max}}{D_0} \quad (1)$$

where D_{max} is the maximum circular contour diameter of HAZ on the surface of the material, D_0 is the diameter of the through hole, as shown in Fig.2(c) and (d).

To ensure that the HAZ from laser processing is completely removed during the side-milling reaming stage, the F_d value should not exceed the ratio of the prefabricated hole diameter to the base hole diameter, which is 1.667. The change of F_d with laser parameters under different parameters is shown in Fig.3. The range of F_d at the entrance of CFRP hole is 1.367-1.612, and at the exit of TC4 hole is 1.301-1.599, which can ensure that HAZ is completely removed in the subsequent reaming stage. From the Fig.3, the HAZ

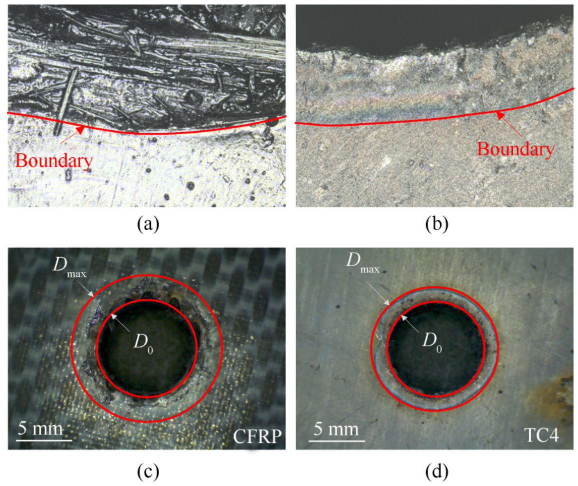

Fig. 2 Characterization diagram of thermal damage area around hole.

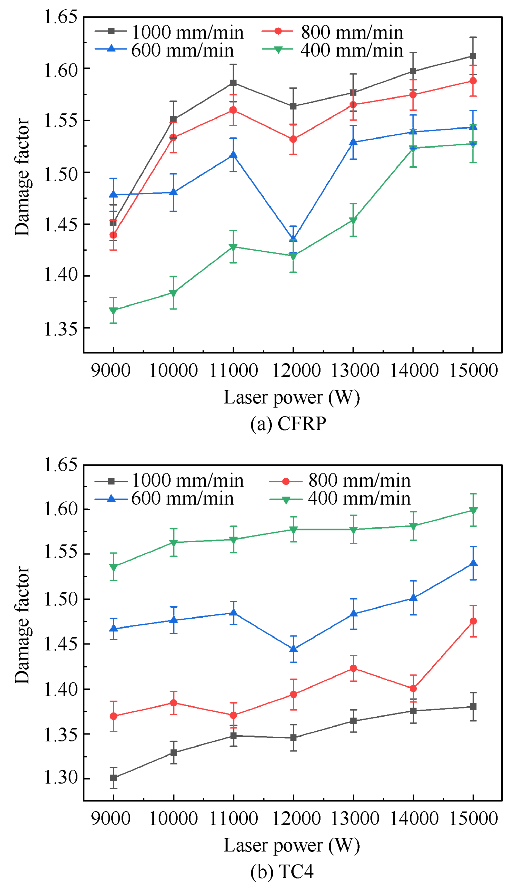

Fig. 3 Variation trend of F_d at hole for CFRP/TC4 laminated stacks.

of both CFRP and TC4 increases as laser power increase. This is because higher laser power results in more energy be absorbed by the material, which leads to higher temperatures in the processing area, and thus a larger HAZ. Therefore, the HAZ increases with the increase of laser power.

The effect of cutting speed on the HAZ is more complex, as changes in cutting speed simultaneously affect the duration of both the laser and assist gas, which have opposing effects on the HAZ. The cooling effect of the assist gas during processing is primarily influenced by the distance between the workpiece and the nozzle, the kerf width, the gas pressure, and the thickness of the workpiece. On the top surface of the CFRP workpiece, where is closest to the laser cutter nozzle, the kerf is widest and the gas pressure is strongest, resulting in the best cooling effect. Conversely, the cooling effect is poorest at the bottom of the TC4 workpiece. As the cutting speed decreases, the duration of the laser and the assist gas increases. On one hand, the CFRP surface benefits from excellent cooling, which causes the laser energy to dissipate quickly. As a result, a longer duration time leads to a smaller HAZ, as shown in Fig.3(a). On the other hand, the poor cooling effect on the TC4 workpiece leads to more noticeable heat accumulation. Consequently, a longer duration time leads to a larger HAZ, as shown in Fig.3(b).

To ensure that the HAZ in both stacks is completely removed during the side-milling reaming stage, the laser power of 12000 W and the cutting speed of 600 mm/min were selected as the laser parameters for subsequent experiments to create the base holes.

3.2. Effect of HAZ on Cutting Force

To investigate the effect of the HAZ on cutting force, cutting forces during the milling process were measured. Since the cutting forces for CFRP are relatively small, the cutting depth for CFRP was fixed at 2.0 mm for this part of the experiment.

The experimental results are shown in Fig.4. The cutting process is divided into three stages. The first stage represents milling the material within 0 to 1 mm from the kerf. In this region, the CFRP matrix is vaporized, and the fibers are highly carbonized, while the TC4 material is severely oxidized, with numerous cracks and pores. The overall strength of the material decreases significantly, resulting in brittle fracture during cutting. Therefore, the cutting force in this stage is the smallest. The second stage represents milling the material within 1 to 2 mm from the kerf. In this region, only the areas close to the kerf are affected by the laser, leading to changes in material properties. The third stage represents milling the material within 2 to 3 mm from the kerf. In this region, the material properties remain largely unchanged. The cutting force in this stage is the largest. Overall, the closer the material is to the kerf, the more severely it is damaged, resulting in smaller cutting forces.

In each stage, a stable milling period was selected, and the average cutting force during the stable milling period was taken as the mean cutting force for that stage. The average cutting forces in the first stage during the processing of CFRP and TC4 were 14.433 N and 36.546 N, respectively. The average cutting forces in the third stage are 36.791 N and 55.209 N, respectively. The introduction of laser energy, resulting in the formation of the HAZ, caused the average cutting force for CFRP to decrease by 60.8%, and by 66.2% for TC4.

To investigate the effect of HAZ severity on cutting force, three sets of laser parameters were used to make the base holes, and material within 1.0 mm of the kerf is removed under the same milling conditions. Changes in cutting force are shown in Fig.5. As laser cutting speed increases, the milling force for CFRP decreases, while the milling force for TC4 increases. Referring to Fig.3, as laser cutting speed increases, the extent of damage to CFRP increases, while it decreases for TC4. Therefore, the closer the material is to the kerf or the more severe the HAZ caused by the laser, the more thoroughly material properties are disrupted, resulting in smaller cutting forces.

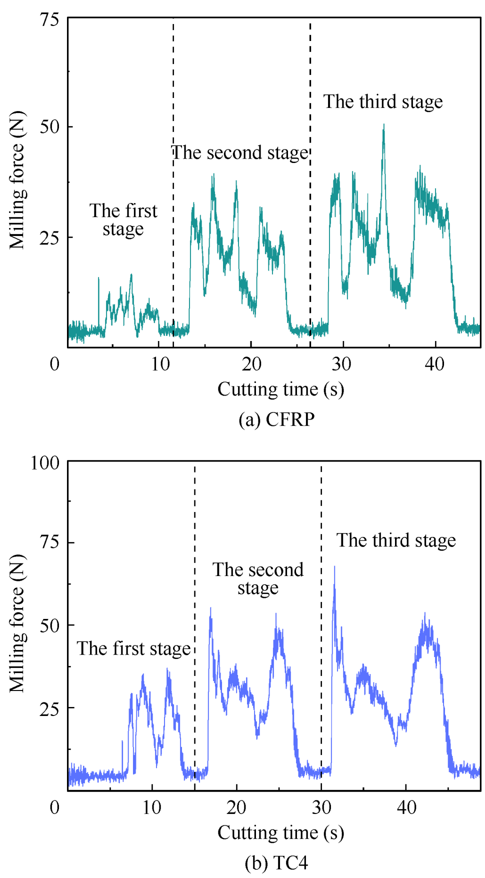

Fig. 4 Effect of HAZ on milling forces in CFRP/TC4 laminated stacks.

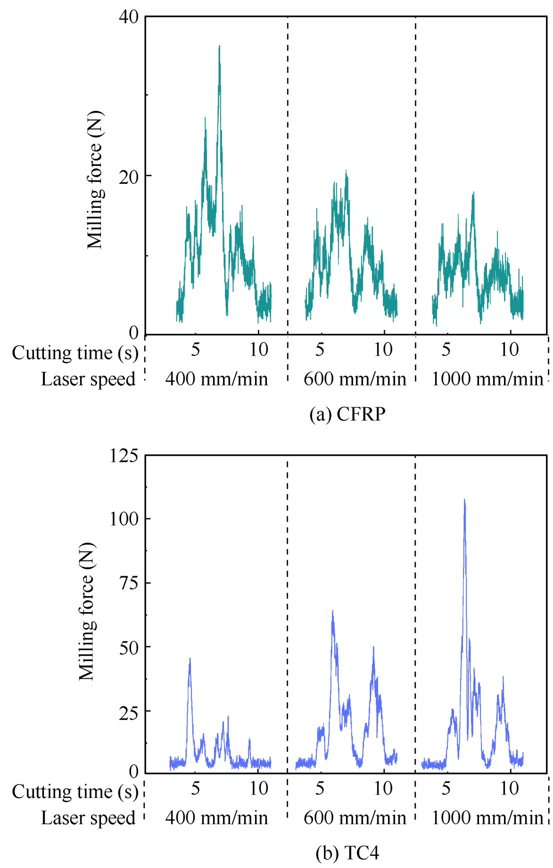

Fig. 5 Effect of laser parameters on milling force in CFRP/TC4 laminated stacks.

3.3. Quality analysis of hole wall

Fig. 6 shows the microscopic surface morphology of the hole walls after side-milling reaming with and without MQL. During dry cutting, the CFRP surface exhibits pits caused by fiber pull-out, while the TC4 surface contains numerous pits, cracks and adhesive particles among other defects caused by built-up edge. Furthermore, the introduction of MQL significantly improves the surface quality of the hole walls in both CFRP and TC4 stacks, resulting in smooth surfaces with no obvious defects. To quantitatively analyze the differences in the processed surfaces under dry cutting and MQL conditions, surface roughness (Sa) is used to characterize and analyze the quality of the hole wall surfaces.

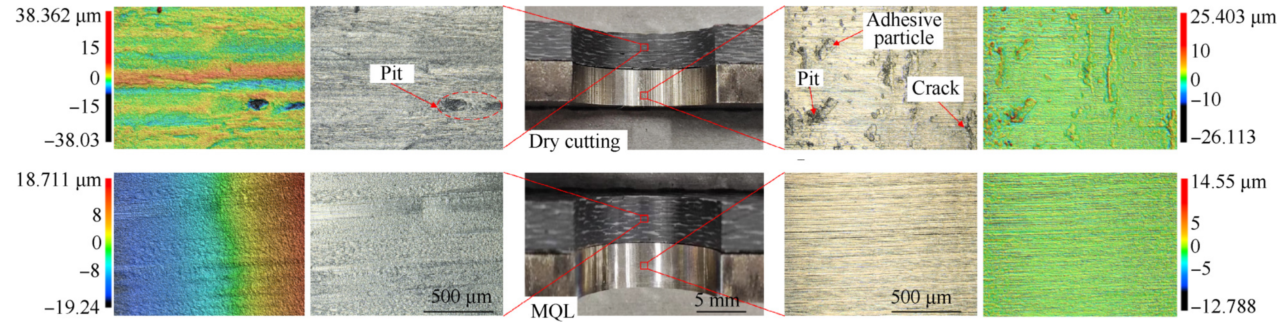

Fig. 6 Surface microstructure of hole wall of laser and side-milling compound drilling.

The influence of processing parameters on the Sa of the hole walls for CFRP and TC4 is shown in Fig. 7. It can be observed that under the same parameters, the surface quality with MQL is superior to that of dry cutting. The introduction of MQL results in a maximum improvement of 36.1% in the surface quality for CFRP and 36.8% for TC4. This is due to the cooling and lubrication effects of MQL during processing, which enhance the stability of the process and reduce the likelihood of built-up edge formation when cutting TC4, thereby improving surface quality.

In Fig. 7(a) and (b), under dry cutting conditions, the Sa values for both CFRP and TC4 show an upward trend as the increase in spindle speed. This is because the increase in spindle speed effectively reducing the cutting force and improving processing stability, but also leading to a significant rise in cutting temperature. On one hand, the higher temperature causes greater debonding in CFRP, leading to a higher Sa value. On the other hand, it increases the likelihood of built-up edge formation and induces higher thermal and mechanical stresses, which result in more adhesion particles, scratches, and cracks on the TC4 surface, thereby increasing the Sa value. Under MQL conditions, due to the excellent cooling and lubricating properties of the oil mist, the cutting temperature is significantly reduced, resulting in a decrease in the Sa values for both CFRP and TC4 surfaces.

Fig. 8(a) and (b) illustrate the variation in Sa with axial cutting

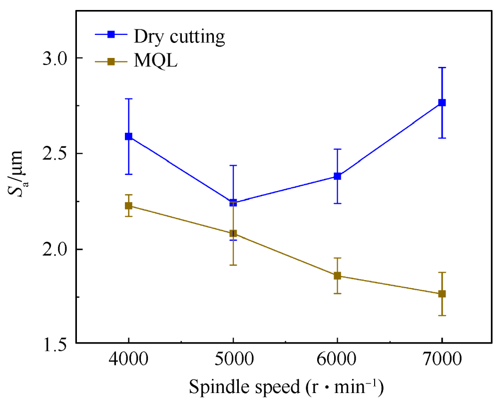

(a) CFRP

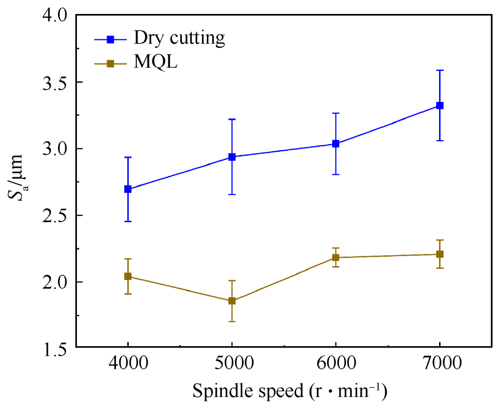

(b) TC4

Fig. 7 Effect of spindle speed on Sa

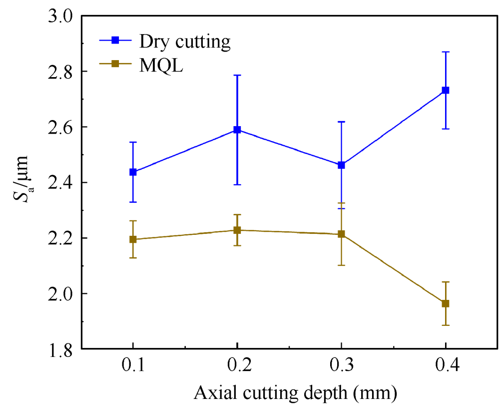

(a) CFRP

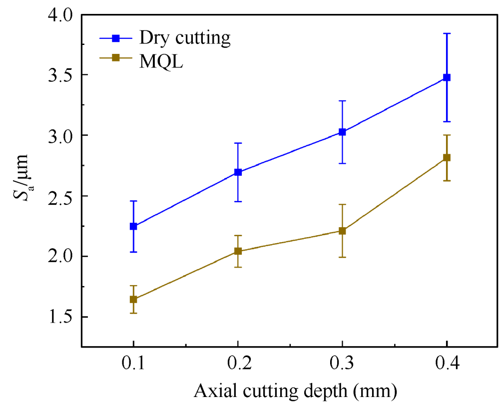

(b) TC4

Fig. 8 Effect of axial cutting depth on Sa.

depth. The Sa value for CFRP fluctuates as axial cutting depth increase, but the fluctuations are minor. For TC4, the Sa value increases significantly as axial cutting depth increase. On one hand, the increase in axial cutting depth leads to higher cutting force, destabilizing the weakly rigid robotic processing system , resulting in increased surface roughness. On the other hand, the increase in axial cutting depth diminishes the coverage ability of the oil mist, reducing the cooling and lubrication effects of MQL, and deteriorate surface quality.

3.4. Comparative analysis of interlayer burrs

Fig.9 shows the three-dimensional imaging of the interlayer burr captured by the laser microscope, with the unprocessed surface used as a reference plane for measuring the burr height. Then the burr height can be directly read using KEYENCEVK-X100 software. It can be observed that the CFRP burr is very small, measuring only 26.573μm. This is because the TC4 provides a structural support for the CFRP, making it easier to cut the carbon fibers, resulting in a smaller burr.

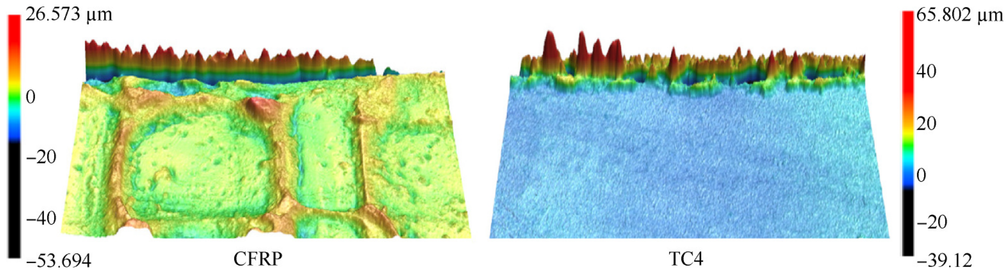

Fig. 9 Three-dimensional imaging of CFRP and TC4 interlayer burrs.

Fig. 10 shows the comparison of the experimental results of the interlayer burr height with different processing parameters. It can be observed that the interlayer burr height of both CFRP and TC4 decreases as spindle speed increases. The main reason is that higher spindle speed reduces milling force, which has a positive impact on the reduction of burr height. The effect of cutting depth on burr height is shown in Fig.10(b). The experimental results indicate that the burr height of both CFRP and TC4 increases with the increase of cutting depth. This trend is caused by the greater cutting depth, which results in more material being removed. This ultimately leads to a corresponding increase in burr volume, thereby deteriorating the burr height.

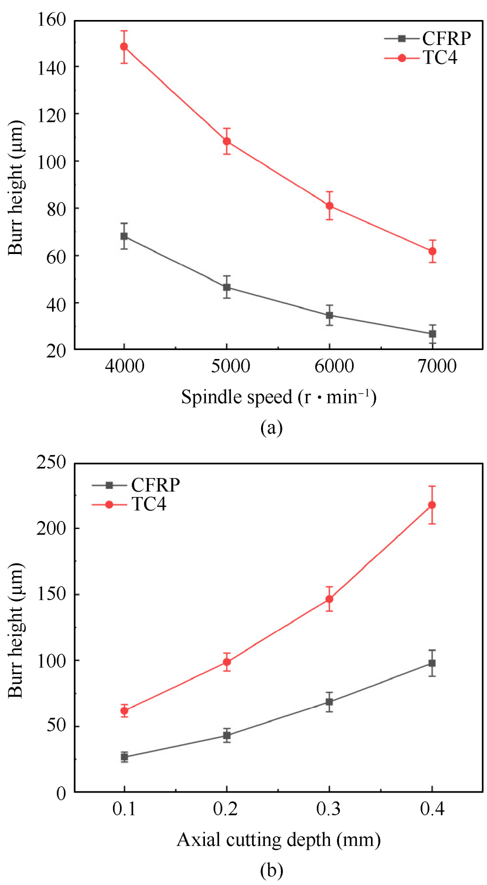

Fig. 10 Variation trend of interlayer burr height with processing parameters.

The experimental results indicate that under MQL conditions, within the selected parameter range, the hole wall roughness is consistently less than 3.2 μm. The overall processing quality is optimal at a spindle speed of 7000 r/min, a feed rate of 120 mm/min, and a cutting depth of 0.1 mm. Under these conditions, the Sa values for CFRP and TC4 are 1.737 μm and 1.918 μm, respectively, and the interlayer burr heights are 26.734 μm and 60.802 μm, respectively. These values meet the processing quality requirements of the aerospace industry.

4. Conclusion

In this paper, experiments were conducted by laser and side-milling compound technology of drilling for CFRP/TC4 laminated stacks based on the robot. The relationships between the HAZ, cutting forces, and processing quality were investigated. The feasibility of making large holes by laser and side-milling compound technology was validated, and the following conclusions were reached:

(1) The size of the HAZ for both CFRP and TC4 increases with the increase in laser power, but exhibits opposite trends with changes in laser cutting speed. Within the selected laser parameters, the damage factors for both CFRP and TC4 range from 1.301 to 1.612, ensuring that all the damaged material can be completely removed during the side-milling reaming stage.

(2) The experimental results indicate that the HAZ caused by the laser leads to a maximum reduction of 60.8% in the average cutting force for CFRP and a maximum reduction of 66.2% for TC4. Furthermore, the higher degree of thermal damage results in better improvement in cutting forces, which can effectively extend the tool life.

(3) MQL significantly improves the surface quality of the hole walls for both CFRP and TC4, leading to a maximum reduction of 36.1% in the Sa for CFRP and 36.8% for TC4. Under MQL conditions, with a spindle speed of 7000 r/min, a feed rate of 120 mm/min, and a cutting depth of 0.1 mm, the overall machining quality is optimal. Under these conditions, only a few pits and a small num-

ber of pulled-out fibers are observed on the surface of the CFRP, while the surface of the TC4 shows no significant pits or cracks. Additionally, the height of burrs between laminates is minimal.

Acknowledgements

This work was supported by the National Natural Science Foundation of China (No. U22A20204 & No. 52305472).

References

1. Chen C, Zhao Q, Wang A, et al. Experimental study on step drill geometry and pecking drilling with variable parameters processing method as drilling of CFRP and Ti stacks. *J Manuf Process* 2024;117:355-365.
2. Li YX, Jiao F, Zhang ZQ, et al. Research on entrance delamination characteristics and damage suppression strategy in drilling CFRP/Ti6Al4V stacks. *J Manuf Process* 2022;76:518-531.
3. Liu FY, Chen T, Duan ZY, et al. Ultrasonic assisted pecking drilling process for CFRP/Ti laminated stacks. *J Manuf Process* 2023;108:834-851.
4. Cao SP, Li Y, Zhang KF, et al. Investigation of CFRP damages induced by the interface high temperature and mixed tool wear mechanism in drilling of thin-walled CFRP /Ti stacks. *Compos Struct* 2023; 323: 177438.
5. Wang CH, Li PN, Li SJ, et al. Study on the mechanism and performance of longitudinal-torsional ultrasonic vibration assisted drilling CFRP/Ti stack. *J Manuf Process* 2023;92:453-465.
6. Cheng H, Luo B, Liang B, et al. Key issues and development trends of mechanical connection relating to aviation CFRP structure performance. *J Adv Manuf Sci Technol* 2022;2(4):2022016.
7. Dong S, Liao WH, Zheng K, et al. Hole surface strengthening mechanism and riveting fatigue life of CFRP/aluminum stacks in robotic rotary ultrasonic drilling. *Chin J Aeronaut* 2023;36(10):471-484.
8. Miyake YJ, Kondo YS. A study on new machining method applied to a collaborative robot for drilling. *Robot Com-Int Manuf* 2022;78:102409.
9. Li SM, Peng HH, Liu CJ, et al. Nonlinear characteristic and chip breaking mechanism for an axial low-frequency self-excited vibration drilling robot. *Int J Mech Sci* 2022;230:107561.
10. Lee JH, Kim SH, Min BK, et al. Posture optimization in robotic drilling using a deformation energy model. *Robot Com-Int Manuf* 2022;78:102395.
11. Yue CX, Xie ZL, Liu XL, et al. Chatter prediction of milling process for titanium alloy thin-walled workpiece based on EMD-SVM. *J Adv Manuf Sci Technol* 2022;2(2):2022010.
12. Jiao F, Li YX, Niu Y, et al. A review on the drilling of CFRP/Ti stacks: Machining characteristics, damage mechanisms and suppression strategies at stack interface. *Compos Struct* 2023;305:116489.
13. Yang YK, Zheng K, Dong S, et al. Investigation into temperature and its effects on hole wall quality in rotary ultrasonic countersinking of thin-walled CFRP/Al stacks. *J Adv Manuf Sci Technol* 2023; 3(2): 2023002.
14. Xu JY, El Mansori M, Voisin J, et al. On the interpretation of drilling CFRP/Ti6Al4V stacks using the orthogonal cutting method: chip removal mode and subsurface damage formation. *J Manuf Process* 2019; 44:435-447.
15. Xu JY, Lin TY, Li LF, et al. Numerical study of interface damage formation mechanisms in machining CFRP/Ti6Al4V stacks under different cutting sequence strategies. *Compos Struct* 2022;285:115236.
16. Xu K, Yang Y, Feng W, et al. Internal cooling techniques in cutting process: A review. *J Adv Manuf Sci Technol* 2024;4(4):2024013.
17. Dong S, Zheng K, Zhang WT. Investigation on cutting temperature of CFRP in robotic rotary ultrasonic drilling with minimum quantity lubrication. *J Adv Manuf Sci Technol* 2025;5(1):2025001.
18. Wang JL, Ge JY, Chen G, et al. Sustainable cooling/lubrication induced thermo-mechanical effects on ultrasonic vibration helical milling of CFRP/Ti-6Al-4V stacks. *Int J Light Mater Manuf* 2023;6:311-328.
19. Geng DX, Sun ZF, Liu YH, et al. Unravelling the influence of vibration on material removal and microstructure evolution in ultrasonic transversal vibration-assisted helical milling of Ti-6Al-4V holes. *J Mater Process Tech* 2024;326:118320.
20. Pereira RBD, Brando LC, Paiva APD, et al. A review of helical milling process. *Int J Mach Tools Manuf* 2017;120:27-48.
21. Huynh HN, Assadi H, Dambly V, et al, Direct method for updating flexible multibody systems applied to a milling robot. *Robot Comput Integr Manuf* 2021;68:102049.
22. Wu JW, Peng FY, Tang XW, et al. Characterization of milling robot mode shape and analysis of the weak parts causing end vibration. *Measurement* 2022;203:11934.
23. Gautam GD, Pandey AK. Pulsed Nd: YAG laser beam drilling: a review. *Opt Laser Technol* 2018;100:183-215.
24. KUMAR D, GURURAJA S. Investigation of hole quality in drilled Ti/CFRP/Ti laminates using CO_2 laser. *Opt Laser Technol* 2020; 126: 106130.
25. Wu T, Ma YW, Xia HB, et al. Measurement and simulation of residual stresses in laser welded CFRP/steel lap joints. *Compos Struct* 2022; 292:115687.
26. Schmidt B, Rose M, Zimmermann M, et al. Analysis of process-induced damage in remote laser cut carbon fibre reinforced polymers. *J Mater Process Technol* 2021;295:117162.
27. Li HN, Ye YX, Du TT, et al. The effect of thermal damage on mechanical strengths of CFRP cut with different pulse-width lasers. *Opt Laser Technol* 2022;153:108219.
28. Li MJ, Gan GC, Zhang Y, et al. Thermal damage of CFRP laminate in fiber laser cutting process and its impact on the mechanical behavior and strain distribution. *Arch Civ Mech Eng* 2019;19(4):1511-1522.
29. Li WY, Rong YM, Huang Y, et al. Effect of thermal damage on dynamic and static mechanical properties of CFRP short pulse laser hole cutting. *Eng Fract Mech* 2023;286:109306.